Convergence Behavior of DSQ and DSQK Elements for Composite Plates

Pierro Bernard Johan[1] and Imam Jauhari Maknun[2]

[1,2] Civil Engineering Department, Universitas Indonesia, Depok, 16424, Indonesia

Abstract. Computational method in the composite materials application such as bending plate problems is needed since the analytical solutions are only available for simple structures. This paper presents in a unified and comparative manner of solution accuracy for composite plate structures using two quadrilateral plate bending composite elements, i.e. DSQ (Discrete Shear Quadrilateral) and DSQK (modified DSQ) elements which are published in 1990 and 2011 respectively. All the elements have 4 nodes and 5 degrees of freedom per node (three displacements and two rotations), considering transverse shear effects. The plate kinematics is based on Reissner-Mindlin plate theory with discrete shear constraints introduced to relate the kinematical and the independent shear strains. In the DSQK element, the couple between lower order and higher order bending energy is assumed to be zero to fulfil the constant bending patch test. The independent transverse shear strain is expressed only by second derivatives of the rotation obtained from a unified and integrated kinematic relationship, constitutive law, and equilibrium equations. There are valid to for thin to thick composite plates and give good results in isotropic, classical benchmark and patch tests. Two tests proposed with sandwich and 3 and 9 layers are evaluated using uniform mesh and distorted mesh. The convergence of central displacement is then presented to understand which element give better accuracy. The DSQ element gives good convergence behavior to the reference solution. Moreover, both uniform and distorted mesh of DSQ element provides better accuracy than DSQK element for all cases analyzed in this paper.

Keywords: Composite Plates, DSQ, DSQK.

1 Introduction

Composite materials are widely used in civil, mechanical, and aerospace engineering applications [1][2]. Composite material provides high stiffness and strength-to-weight ratio, corrosion, and high-temperature resistance [3]. An effective computational method in the composite application is very expected since the analytical solutions are only available for simple structures. It is well known that the Finite Element Method performs well in computational mechanics [4]. The composite application can be found in references [5][6][7][8]. One of the composite material applications is for plate structures, referred to as bending problems. In the plate bending problems, the Reissner-Mindlin plate is used to formulate many elements capable of being used in thick-to-thin plate structures [9] [10].

The phenomenon of shear locking is one of the big problems in finite element analysis for plate-bending elements. Hughes and Tezduyar proposed the Assumed Natural Strain (ANS) as one of the alternatives to solve the shear locking [11][12]. Many authors use it very effectively to develop a new element. Bathe and Dvorkin proposed

S. C. Asih et al. (eds.), *Proceedings of the 19th International Conference on Quality in Research (QiR 2025)*, Advances in Engineering Research 303,
https://doi.org/10.2991/978-94-6239-717-0_7

a variation of the ANS method, and the well-known MITC element was introduced [13][14][15].

DSQ element was proposed by Batoz and Lardeur in 1990 [16][17]. Using free formulation approach, recently, Katili proposed a modified DSQ element called DSQK [18]. The application of DSQ elements in plate for isotropic and composite structures has been presented in literatures [19][20][21][29][30]. It has been numerically demonstrated that these elements are free from shear locking phenomena. This was further extended to plate and shell for isotropic structures. Regarding the promising results of DSQ and DSQK elements, it is important to continue studying convergence behavior in composite applications. The main objective is to demonstrate convergence behavior on the solution accuracy of the DSQ and DSQK element in composite applications. In numerical simulation, meshing in one of the important steps, both uniform and distorted mesh have been performed in line with the efficiency and accuracy of numerical simulations. Two numerical tests proposed by Srinivas and Pagano are evaluated by using uniform mesh and distorted mesh [22][23][24]. The convergence of central displacement is then presented to understand which element give better accuracy.

2 Introduction

The Reissner-Mindlin (or first order RM) plate theory [25][26] is widely used for the finite element analysis of thin to thick isotropic and composite plates [17].

2.1 Constitutive Equations

In local Cartesian coordinate systems (x, y, z), the constitutive laws for in-plane stresses can be written at each laminate as H_L and G_L refer to Hooke and shear matrix respectively.

$$\left[H_L\right]=\begin{bmatrix} H_{LL} & H_{LT} & 0 \\ & H_{TT} & 0 \\ sym & & G_{LT} \end{bmatrix} \quad (1)\ ; \quad \left[G_L\right]=\begin{bmatrix} G_{LZ} & 0 \\ 0 & G_{TZ} \end{bmatrix} \quad (2)$$

With $H_{LL}=\dfrac{E_L}{1-\upsilon_{LT}\upsilon_{TL}}$ (3) ; $H_{TT}=\dfrac{E_T}{1-\upsilon_{LT}\upsilon_{TL}}$ (4); $H_{LT}=\dfrac{E_L\upsilon_{TL}}{1-\upsilon_{LT}\upsilon_{TL}}$ (5) ;

$E_T\upsilon_{LT}=E_L\upsilon_{TL}$ (6)

The five independent coefficients can be either

H_{LL}, H_{LT}, H_{TT}, $G_{LT}=G_{LZ}$ (7) , G_{TZ} or E_L, E_T, $\upsilon_{LT}\left(\text{or } \upsilon_{TL} \text{with } \upsilon_{LT}=\dfrac{E_T\upsilon_{TL}}{E_L}\right)$ (8)

$G_{LT}=G_{LZ}$ (9), $G_{TZ}\left(\text{or } \upsilon_{TZ} \text{with } G_{TZ}=\dfrac{E_T}{2\left(1+\upsilon_{TZ}\right)}\right)$ (10)

Where E_L is the Young modulus in the fibre direction and E_T is the Young modulus in the transverse direction to the fibre, υ_{LT} and υ_{TL} are the Poisson ratios in the L-T plane of orthotropic layer. The constitutive parameters in matrices $[H_L]$ and $[G_L]$ can be measured experimentally. The orthotropic directions L and T can vary from layer to layer and are represented by angle θ between the local axis x and the directions L_i of the *i-th* layer (Fig. 1). The matrix transformation from orthotropic to local Cartesian coordinates can be written as

$$[R_{L1}] = \begin{bmatrix} C_\theta^2 & S_\theta^2 & C_\theta S_\theta \\ S_\theta^2 & C_\theta^2 & -C_\theta S_\theta \\ -2C_\theta S_\theta & 2C_\theta S_\theta & C_\theta^2 - S_\theta^2 \end{bmatrix} \quad (11) \quad \text{and:} \quad [R_{L2}] = \begin{bmatrix} C_\theta & S_\theta \\ -S_\theta & C_\theta \end{bmatrix} \quad (12)$$

where: $C_\theta = \cos\theta$ (13); $S_\theta = \sin\theta$ (14)

where:

$$[H] = [R_{L1}]^T [H_L][R_{L1}] \quad (15)$$

$$[G] = [R_{L2}]^T [G_L][R_{L2}] \quad (16)$$

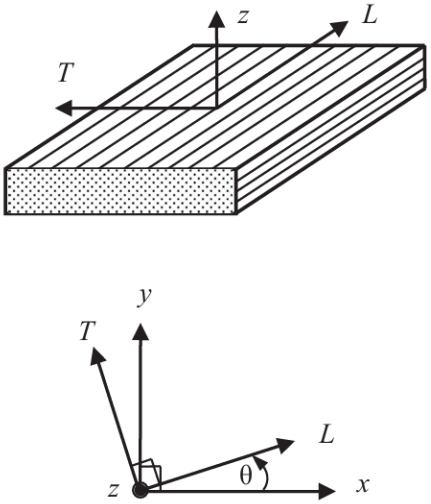

Fig. 1. Orthotropic Plate[27]

2.2 Stress Resultants

For composite structures, the stress resultant constitutive equations are obtained by summing up over different layers. Stress resultant elasticity matrix for membrane and bending parts along with the membrane-bending coupling term due to non-symmetry of the composite plate are obtained, which are denoted as $[H_m]$, $[H_b]$, $[H_{mb}]$ and $[H_s]$ matrices (see Fig. 2).

Membrane constitutive matrix:

$$\left[H_m\right]=\begin{bmatrix} H_{m11} & H_{m12} & H_{m13} \\ & H_{m22} & H_{m23} \\ Sym. & & H_{m33} \end{bmatrix}=\sum_{i=1}^{nl}\left[H\right]_i h_i \tag{13}$$

$$h_i=\left(z_{i+1}-z_i\right) \tag{14}$$

Bending constitutive matrix:

$$\left[H_b\right]=\begin{bmatrix} H_{b11} & H_{b12} & H_{b13} \\ & H_{b22} & H_{b23} \\ Sym. & & H_{b33} \end{bmatrix}=\frac{1}{3}\sum_{i=1}^{nl}\left[H\right]_i\left(z_{i+1}^3-z_i^3\right) \tag{15}$$

Coupled membrane-bending constitutive matrix:

$$\left[H_{mb}\right]=\begin{bmatrix} H_{mb11} & H_{mb12} & H_{mb13} \\ & H_{mb22} & H_{mb23} \\ Sym. & & H_{mb33} \end{bmatrix}=\frac{1}{2}\sum_{i=1}^{nl}\left[H\right]_i h_i \bar{z}_i \tag{16}$$

$$\bar{z}_i=\frac{1}{2}\left(z_{i+1}+z_i\right) \tag{17}$$

where h_i is the layer thickness.

Shear constitutive matrix:

$$\left[\bar{H}_s\right]=\begin{bmatrix} \bar{H}_{s11} & \bar{H}_{s12} \\ Sym. & \bar{H}_{s22} \end{bmatrix}=\sum_{i=1}^{nl}\left[G\right]_i h_i \tag{18}$$

$$\left[H_s\right]=\begin{bmatrix} \kappa_{11}.\bar{H}_{s11} & \kappa_{12}.\bar{H}_{s12} \\ Sym. & \kappa_{22}.\bar{H}_{s22} \end{bmatrix} \tag{19}$$

where κ_{11}, κ_{12}, κ_{22} are the transverse shear correction parameters.

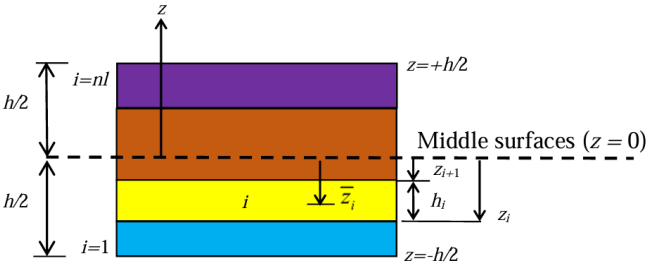

Fig. 2. Definition of Layer in Composite Laminated Shell [28]

3 Formulation of DSQ Element

The detailed formulation of this element has been presented in [21]. By employing the modified Hu-Washizu principle, the strain energy can be expressed as

$$\Pi = \Pi_{int} - \Pi_{ext} \tag{20}$$

$$\Pi_{ext} = \int_A w f_z \, dA \tag{21}$$

$$\Pi_{int} = \Pi_{int}^{m} + \Pi_{int}^{b} + \Pi_{int}^{mb} + \Pi_{int}^{s} \tag{22}$$

With

Membrane energy:

$$\Pi_{\text{int}}^{m} = \frac{1}{2}\int_A \langle e \rangle [H_m] \{e\} \, dA \tag{23}$$

Bending energy:

$$\Pi_{\text{int}}^{b} = \frac{1}{2}\int_A \langle \chi \rangle [H_b] \{\chi\} \, dA \tag{24}$$

Membrane bending energy:

$$\Pi_{\text{int}}^{mb} = \frac{1}{2}\int_A \langle e \rangle [H_{mb}] \{\chi\} \, dA + \frac{1}{2}\int_A \langle \chi \rangle [H_{mb}] \{e\} \, dA \tag{25}$$

Shear energy:

$$\Pi_{\text{int}}^{s} = \frac{1}{2}\int_A \langle \underline{\gamma} \rangle [H_s] \{\underline{\gamma}\} \, dA \tag{26}$$

The membrane strain e and curvature χ are given by:

$$\{e\} = \begin{Bmatrix} u_{,x} \\ v_{,y} \\ u_{,y} + v_{,x} \end{Bmatrix} \tag{27}$$

$$\{\chi\} = \begin{Bmatrix} \beta_{x,x} \\ \beta_{y,y} \\ \beta_{x,y} + \beta_{y,x} \end{Bmatrix} \tag{28}$$

The displacement u, v, w, and rotation fields β_x and β_y (Fig. 3) are interpolated as follows:

$$u = \sum_{i=1}^{4} N_i u_i \quad (29); \quad v = \sum_{i=1}^{4} N_i v_i \quad (30); \quad w = \sum_{i=1}^{4} N_i w_i \quad (31)$$

$$\beta_x = \sum_{i=1}^{4} N_i \beta_{x_i} + \sum_{k=5}^{8} P_k C_k \Delta\beta_{s_k} \quad (32)$$

$$\beta_y = \sum_{i=1}^{4} N_i \beta_{y_i} + \sum_{k=5}^{8} P_k S_k \Delta\beta_{s_k} \quad (33)$$

C_k and S_k are the cosines direction defined in Fig. 4.

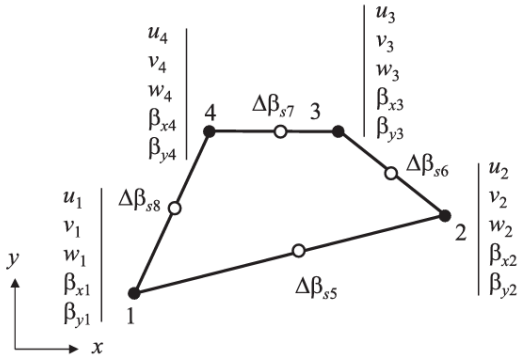

Fig. 3. Kinematic of DSQ Element with 5 DOF's per Node [27]

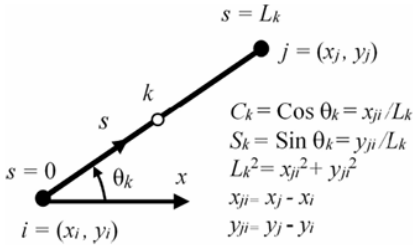

Fig. 4. Cosine Direction on the side i-j [27]

In the DSQ element, the value is independent of shear strains $\underline{\gamma}$ is defined by the equilibrium equations and constitutive equations. $\underline{\gamma}$ is defined in terms of the nodal variables:

$$\left\{\underline{\gamma}\right\} = \begin{Bmatrix} \underline{\gamma}_x \\ \underline{\gamma}_y \end{Bmatrix} = \left[B_{s_\beta}\right]\left\{u_n\right\} + \left[B_{s_{\Delta\beta}}\right]\left\{\Delta\beta_{s_n}\right\} \quad (34)$$

With

$$\left[B_{s_\beta}(\xi,\eta)\right] = \left[\underline{H}_s\right]\left[T_j(\xi,\eta)\right]\left[T_\beta\right] \quad (35)$$

$$\left[B_{s_{\Delta\beta}}(\xi,\eta)\right] = \left[\underline{H}_s\right]\left[T_j(\xi,\eta)\right]\left[T_{\Delta\beta}(\xi,\eta)\right] \quad (36)$$

With $[\underline{H}_s]$ is defined

$$\left[\underline{H}_s\right]=\frac{D_b}{D_s}\begin{bmatrix}1 & \frac{1-\upsilon}{2} & 0 & 0 & 0 & \frac{1+\upsilon}{2}\\ 0 & 0 & \frac{1+\upsilon}{2} & \frac{1-\upsilon}{2} & 1 & 0\end{bmatrix} \quad (37);$$

$$D_b=\frac{Eh^3}{12\left(1-\upsilon^2\right)} \quad (38); \quad D_s=\kappa Gh \quad (39)$$

$$\left[T_j\left(\xi,\eta\right)\right]=\begin{bmatrix}\left[t_j\right] & [0]\\ [0] & \left[t_j\right]\end{bmatrix} \quad (40);$$

$$\left[t_j\right]=\begin{bmatrix}j_{11}^2 & j_{12}^2 & 2j_{11}j_{12}\\ j_{21}^2 & j_{22}^2 & 2j_{21}j_{22}\\ j_{11}j_{21} & j_{12}j_{22} & j_{11}j_{22}+j_{12}j_{21}\end{bmatrix} \quad (41)$$

j_{11}, j_{12}, j_{21} and j_{22} are the components of the inverse Jacobian matrix.

4 Formulation of DSQK Element

The detailed formulation of this element has been presented in [18]. Here, the formulation is recalled briefly. The DSQK is developed using the free formulation approach in attempt to amend the shortcoming of DSQ, which fails to satisfy the constant bending patch test in thick plate cases. In formulating DSQK, assumption that is taken that the *c*-order bending energy is spurious and responsible for the inability of DSQ to fulfil the RM plate theory constant bending patch test. For this reason, the orthogonality condition is forced to the DSQK by considering the zero-coupling stiffness, as follows.

$$\left[k_{b_{u\Delta}}\right]=\left[k_{b_{u\Delta}}\right]=[0] \quad (42)$$

Hence, for the DSQK element, the independent shear strains become

$$\left\{\underline{\gamma}\right\}=\begin{Bmatrix}\underline{\gamma}_x\\ \underline{\gamma}_y\end{Bmatrix}=\left[B_{s_\Delta}\right]\left\{\Delta\beta_n\right\} \quad (43)$$

With

$$\left\{\Delta\beta_n\right\}=\left[A_n\right]_{DSQK}\left\{u_n\right\} \quad (44)$$

Where

$$\left[A_n\right]_{DSQK}=\left[A_\Delta\right]^{-1}\left[A_u\right]_{DSQK} \quad (45)$$

Thus, following equations are obtained

$$\left\{\chi\right\}=\left[B_b\right]_{DSQK}\left\{u_n\right\} \quad (46); \quad \left[B_b\right]_{DSQK}=\left[B_{b_u}\right]+\left[B_{b_\Delta}\right]\left[A_n\right]_{DSQK} \quad (47)$$

$$\left\{\underline{\gamma}\right\} = \left[B_s\right]_{DSQK} \left\{u_n\right\} \quad (48); \quad \left[B_s\right]_{DSQK} = \left[B_{s_\Delta}\right]\left[A_n\right]_{DSQK} \quad (49)$$

Hence, bending and shear stiffness

$$\left[k_b\right] = \left[k_{b_u}\right] + \left[A_n\right]^T_{DSQK} \left[k_{b_\Delta}\right]\left[A_n\right]_{DSQK} \quad (50)$$

$$\left[k_s\right] = \int_A \left[B_s\right]^T_{DSQK} \left[H_s\right]\left[B_s\right]_{DSQK} dA \quad (51)$$

The total stiffness matrix of the DSQK element is the summation of bending and shear stiffness.

5 Research Methodology

To compare the solution accuracy of the DSQ and DSQK elements in a composite plate structure, 2 cases will be analyzed that previously gives analytical result so that result can be compared with numerical result. The first is a simply supported (SS) sandwich plate proposed by Srinivas [22], and the second is a three- and nine-layer SS plate proposed by Pagano [24]. The results of convergence are presented in central displacement. Two mesh are evaluated to understand the effect of mesh on the accuracy of the solution. Uniform mesh and distorted mesh are used in this paper.

6 Result and Discussion

To compare the solution accuracy of the DSQ and DSQK elements in a composite plate structure, 2 cases will be analyzed that previously gives analytical result so that result can be compared with numerical result. The first is a simply supported (SS) sandwich plate proposed by Srinivas

6.1 Srinivas Sandwich Plate

Figure 5 shows the geometric details of the simply supported (SS) sandwich plate proposed by Srinivas. Due to the symmetry condition, only the area of ABCD is analyzed. The material properties are: E_L = 3.4156 MPa; E_T = 1.7931 MPa; υ_{LT} = 0.44; G_{LT} = 1 MPa; G_{LZ} = 0.608 MPa; G_{TZ} = 1.015 MPa. The three layers of a 0/0/0 (each number refer to fiber orientation) symmetrical sandwich plate with the boundary condition w=β_s=0 on the boundary of the plate are evaluated. In this test, three condition are used, C=1, C=10, and C=50, where C is the factor proportionality of layer 2 (core) and layers 1 and 3 (skin). Each factor has each shear correction factor (κ_{11}, κ_{22} and κ_{12}) that presented in tables below.

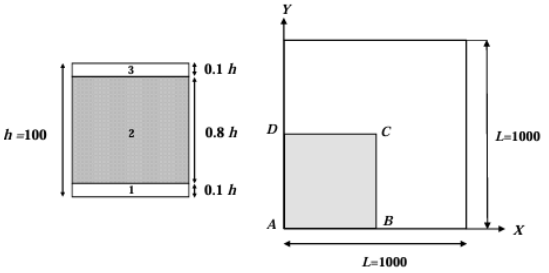

Fig. 5. SS Sandwich Plate [28]

The results of the central deflection at point C are presented for two different mesh. The convergences are studied when the number of mesh (N) are increased. The analytical solutions are used as reference solutions. In this test, the central displacement is expressed as:

$$\underline{w}_c = \frac{w_c G_{LT}(\text{Core})}{hf_z} \tag{52}$$

Table 1. The central deflections w_c.

NxN	C=1		C=10		C=50	
	$\kappa_{11}= \kappa_{22}=0.8333$; $\kappa_{12}=0$		$\kappa_{11}= \kappa_{22}=0.3521$; $\kappa_{12}=0$		$\kappa_{11}= \kappa_{22}=0.0938$; $\kappa_{12}=0$	
	DSQ	DSQK	DSQ	DSQK	DSQ	DSQK
4x4	181.47	184.76	42.122	42.748	16.95	17.095
8x8	181.39	182.21	42.029	42.185	16.865	16.902
16x16	181.36	181.57	42.006	42.045	16.845	16.854
32x32	181.36	181.41	42	42.01	16.839	16.842
64x64	181.36	181.37	41.998	42.001	16.838	16.839
Srinivas	181.05		41.91		16.75	

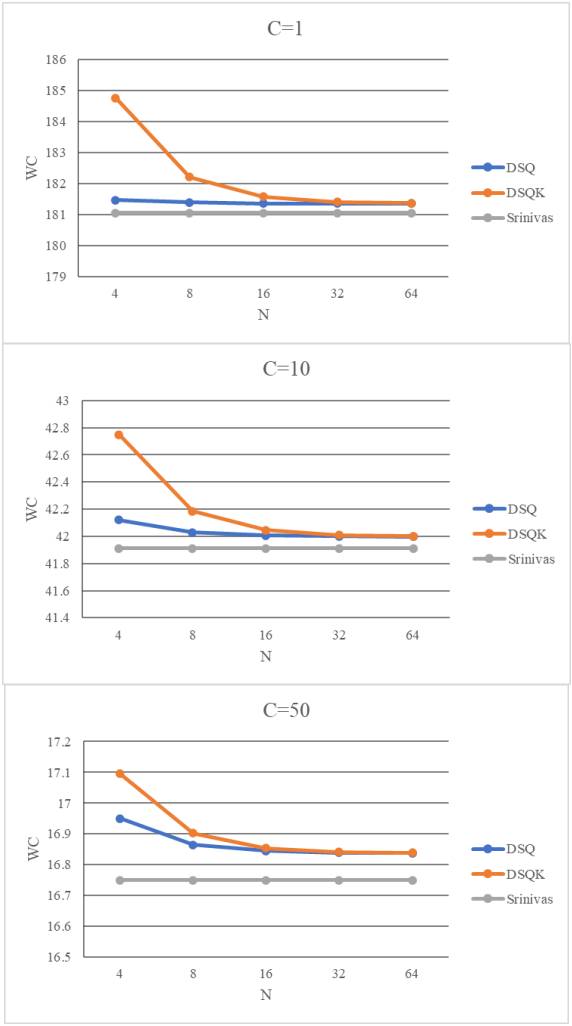

Fig. 6. The central deflection w_c

Table 1 and Figure 6 present the results for uniform mesh. The results given by DSQ and DSQK are close to the proposed solution. Also, the results of DSQ element converge faster than DSQK element. Again, DSQ element performs better than DSQK element. Starting from 16x16 element, element DSQ and DSQK give almost similar results.

Table 2. The central deflections w_c distorted mesh

NxN	C=1		C=10		C=50	
	$\kappa_{11}= \kappa_{22}=0.8333$; $\kappa_{12}=0$		$\kappa_{11}= \kappa_{22}=0.3521$; $\kappa_{12}=0$		$\kappa_{11}= \kappa_{22}=0.0938$; $\kappa_{12}=0$	
	DSQ	DSQK	DSQ	DSQK	DSQ	DSQK
4x4	184.21	188.53	42.582	43.614	17.027	17.416
8x8	182.03	183.09	42.133	42.381	16.88	16.97
16x16	181.51	181.78	42.031	42.092	16.848	16.87
32x32	181.39	181.46	42.006	42.021	16.84	16.846
64x64	181.36	181.38	42	42.004	16.838	16.84
Srini-vas	181.05		41.91		16.75	

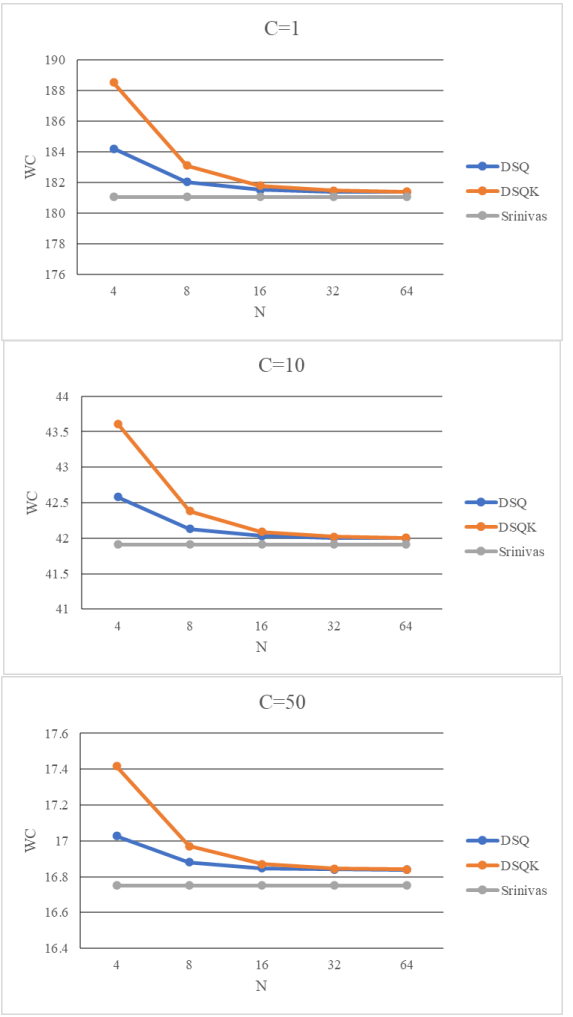

Fig. 7. The central deflection w_c distorted mesh

Table 2 and Figure 7 present the results for central displacement for distorted mesh. The two elements give the results close to the reference solution. Moreover, element DSQ performs better than element DSQK for small number of elements. To conclude, the DSQ element is not sensitive to mesh distortion and give convergence result better than DSQK element.

6.2 The 3 and 9 Layers SS Plate

Figure 8 presents the details of three and nine-layer square plates proposed by Pagano. The uniform and distorted mesh are evaluated by varying *L/h* ratio (*L/h*=4,10,50,100). The material properties used in this test are E_L = 25 MPa; E_T = 1 MPa; υ_{LT} = 0.25; G_{LT} = 0.5 MPa; G_{TZ} = 0.2 MPa. The shear correction factor for 3-layer case: κ11 = 0.570; κ22 = 0.882; κ12 = κ21= 0 and stratification 0/90/0 symmetrical. While for 9-layer case, the shear correction factor are κ11 = 0.670; κ22 = 0.666; κ12 = κ21= 0 and stratification 0/90/0/90/0/90/0/90/0 symmetrical. The boundary conditions are w = β_s = 0 on the plate boundary. The sinusoidal loading $f_z = f_0 \sin(\pi x/L)\sin(\pi y/L)$ is applied to the structures. The convergence behavior is presented in the form of vertical displacement in point C, which is expressed as:

$$\underline{w}_C = \frac{\pi^4 w Q}{12 S^4 h f_0}; Q = 4G_{LT} + \left[E_L + E_T(1+2\upsilon_{TT})\right]/(1-2\upsilon_{LT}\upsilon_{TL}) \tag{53}$$

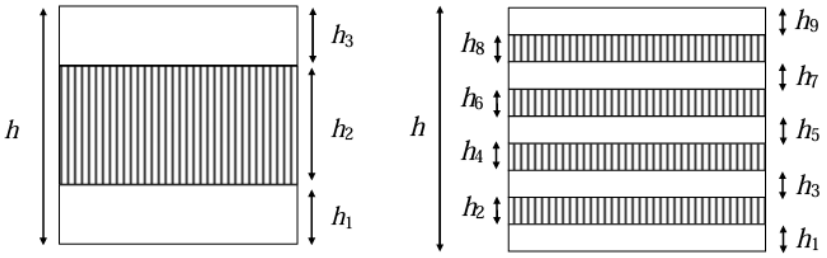

Fig. 8. The 3 and 9 layers[28]

Table 3. The central deflections w_c (3 layers)

NxN	3-layer							
	L/h = 4		*L/h* = 10		*L/h* = 50		*L/h* = 100	
	DSQ	DSQK	DSQ	DSQK	DSQ	DSQK	DSQ	DSQK
4x4	4.806	4.812	1.753	1.757	1.034	1.036	1.009	1.012
8x8	4.776	4.777	1.747	1.748	1.034	1.034	1.009	1.010
16x16	4.768	4.768	1.746	1.746	1.034	1.034	1.009	1.010
32x32	4.766	4.766	1.745	1.745	1.034	1.034	1.009	1.009
64x64	4.766	4.766	1.745	1.745	1.034	1.034	1.009	1.009
Ref.	4.491		1.709		1.031		1.008	

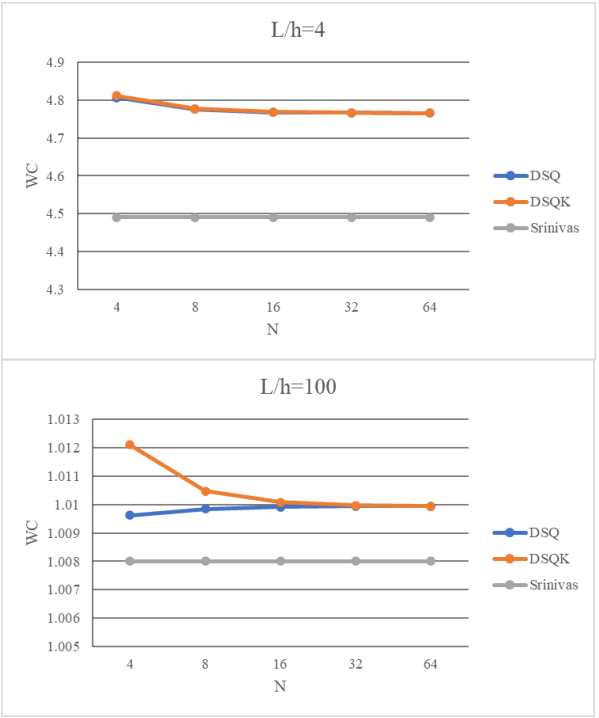

Fig. 9. The central deflection w_c (3 layers)

Table 4. The central deflections w_c (9 layers)

NxN	**9-layer**							
	L/h = 4		*L/h* = 10		*L/h* = 50		*L/h* = 100	
	DSQ	DSQK	DSQ	DSQK	DSQ	DSQK	DSQ	DSQK
4x4	4.218	4.220	1.523	1.526	1.022	1.024	1.006	1.009
8x8	4.187	4.188	1.519	1.519	1.022	1.023	1.006	1.007
16x16	4.180	4.180	1.517	1.518	1.022	1.022	1.007	1.007
32x32	4.178	4.178	1.517	1.517	1.022	1.022	1.007	1.007
64x64	4.177	4.177	1.517	1.517	1.022	1.022	1.007	1.007
Ref.	4.079		1.512		1.021		1.005	

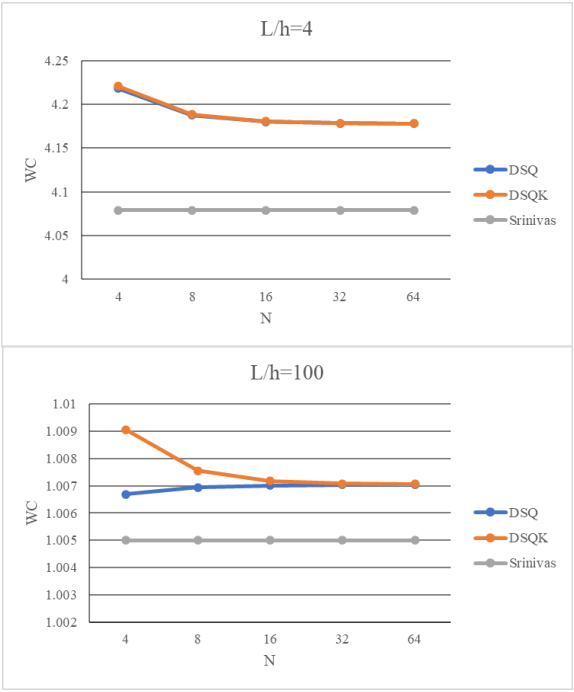

Fig. 10. The central deflection w_c (9 layers)

Table 3 and Table 4 show the results of central displacement for 3-layer and 9-layer cases for different values of *L/h*. The results were very close to the reference solution. Figure 9 and Figure 10 present the convergence behavior for *L/h* = 4 and 100. DSQ element performs better than DSQK element. DSQ element performs better than DSQK element for coarse mesh (small number of elements). It is essential to use element DSQ for coarse element to get accurate results.

Table 5. The central deflections w_c (3 layers distorted mesh)

NxN	**3-layer**							
	L/h = 4		*L/h* = 10		*L/h* = 50		*L/h* = 100	
	DSQ	DSQK	DSQ	DSQK	DSQ	DSQK	DSQ	DSQK
4x4	4.843	4.818	1.765	1.772	1.051	1.048	1.027	1.024
8x8	4.779	4.775	1.749	1.751	1.037	1.037	1.014	1.013
16x16	4.768	4.768	1.746	1.746	1.035	1.034	1.010	1.010
32x32	4.766	4.766	1.745	1.745	1.034	1.034	1.010	1.010
64x64	4.766	4.766	1.745	1.745	1.034	1.034	1.009	1.009
Ref.	4.491		1.709		1.031		1.008	

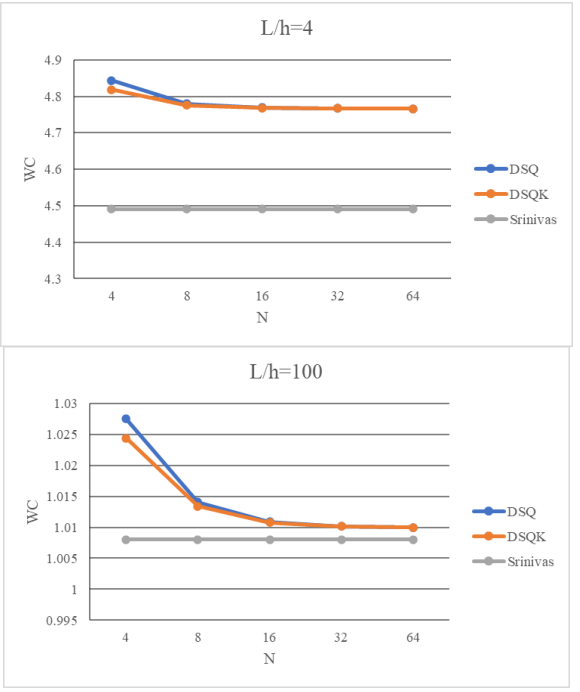

Fig. 11. The central deflection w_c (3 layers distorted mesh)

Table 6. The central deflections w_c (9 layers distorted mesh)

NxNx2	9-layer							
	L/h = 4		*L/h* = 10		*L/h* = 50		*L/h* = 100	
	DSQ	DSQK	DSQ	DSQK	DSQ	DSQK	DSQ	DSQK
4x4x2	4.212	4.230	1.532	1.533	1.033	1.033	1.018	1.017
8x8x2	4.184	4.188	1.521	1.520	1.025	1.025	1.009	1.009
16x16x2	4.179	4.180	1.518	1.518	1.023	1.023	1.007	1.007
32x32x2	4.178	4.178	1.517	1.517	1.022	1.022	1.007	1.007
64x64x2	4.177	4.177	1.517	1.517	1.022	1.022	1.007	1.007
Ref.	4.079		1.512		1.021		1.005	

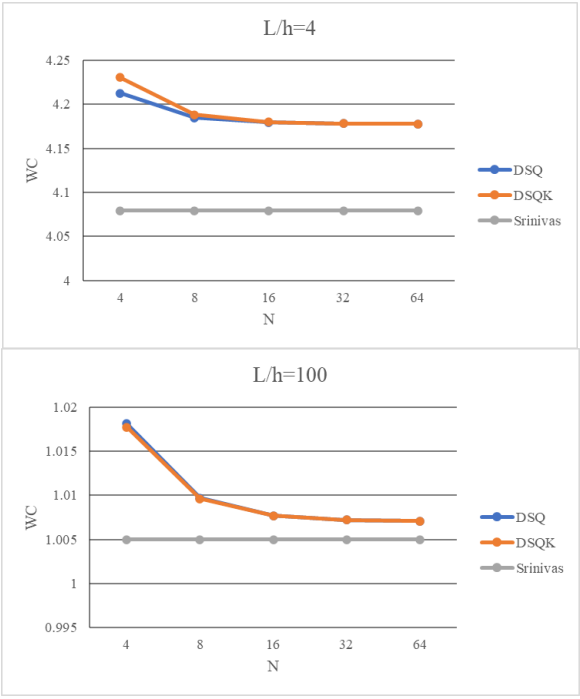

Fig. 12. The central deflection w_c (9 layers distorted mesh)

The test is performed using distorted mesh, presenting the result in Tables 5-6 and Figures 11-12. The results are also compared with the solution proposed by Pagano. The DSQ and DSQK elements give good results that converge to the reference solutions. From the result, DSQ element gives better results than DSQK element.

7 Conclusion

The comparison of DSQ and DSQK elements has been presented in two different cases. The results showed that the DSQ and DSQK elements give good convergence behavior compared to the reference solution proposed by Srinivas and Pagano. Starting from 16x16 element (small number of elements), the result given by DSQ and DSQK are close to the reference solution. In addition, the DSQ element perform better than DSQK element. For all tests using distorted mesh, the DSQ and DSQK elements give convergence results as uniform mesh. Moreover, It is found that DSQ element performs better than DSQK element for coarse mesh (small number of elements). Both DSQ and DSQK elements give similar results when the number of elements increases (starting from 16x16). It is found that the element strategy is an essential factor in determining the accuracy of numerical simulation. Finally, the DSQ element can be used as an alternative element to analyze composite plate structures.

Acknowledgments. The financial support from Engineering Faculty Universitas Indonesia are gratefully acknowledged.

Disclosure of Interests. The authors declare that they have no known competing financial interests or personal relationships that could have appeared to influence the work reported in the paper.

References

1. Nayak S, Kumar M.P. Mechanical Characterization and Static Analysis of Natural Fiber Based Composite Propeller Blade. Evergreen, 10(2), p.805-812, 2023. https://doi.org/5109/6792832.
2. Bhati B., Rath A., Bector K., Ahmad S., Singari R.M. Recent Developments in the use of Composites for Knee Cap Prosthetics. Evergreen, 10(2), p.1084-1093,2023. https://doi.org/10.5109/6793667.
3. Li Q, Chen S. A linear smoothed quadratic finite element for buckling analysis of laminated composite plates. Eng Anal Bound Elem, 163, p.345-354,2024. https://doi.org/10.1016/j.enganabound.2024.03.023.
4. Huang L. L., Sheikh A.H., Ng C.T., Griffith M. C. An efficient finite element model for buckling analysis of grid stiffened laminated composite plates. Composite Structures, 122, p. 41-50, 2015. https://doi.org/10.1016/j.compstruct.2014.11.039.
5. Kumar A., Chandra A.K., Angra S. Optimization of Stiffness Properties of Composite Sandwich using Hybrid Taguchi-GRA-PCA. Evergreen, 8(2), p.310-317, 2021. https://doi.org./10.5109/4480708.
6. Kumar A,, Chandra A.K., Angra S. Numerical Modelling of a Composite Sandwich Structure Having Non Metallic Honeycomb Core. Evergreen, 8(4), p.759-767, 2021. https://doi.org/10.5109/4742119.
7. Gupta A., Kumar H., Nagdeve L., Arora P.K., EDM Parametric Study of Composite Materials: A Review. Evergreen, 7(4), p.519-529, 2020. https://doi.org/10.5109/4150741.
8. Ismaiel A.M.M., Metwalli S.M., Elhadidi M.N., Yoshida S. Fatigue Analysis of an Optimized HAWT Composite Blade. Evergreen, 4(2/3), p.1-6, 2017. https://doi.org/10.5109/1929656.
9. Reissner E., The effect of transverse shear deformation on the bending of elastic plates. Journal of Applied Mech in Engineering ASME, 12(2), p.69-77, 1945. https://doi.org/10.1115/1.4009435.
10. Mindlin R.D. Influence of rotator inertia and shear on flexural motion of isotropic elastic plates. J.Appl.Mech, 18, p.31-38, 1951. https://doi.org/10.1115/1.4010217.
11. Hughes T.J.R, Tezduyar T.E. Finite el. based upon Mindlin plate theory with particular reference to the 4-node bilinear isoparametric el. J App. .Mech., 48(3), p.587-596, 1981. https://doi.org/10.1115/1.3157679.
12. MacNeal R.H. Derivation of element stiffness matrices by assumed strain distributions. Nucl. Eng. Des., 70(1), p.3-12, 1982. https://doi.org/10.1016/0029-5493(82)90262-X.

13. Dvorkin E.N., Bathe K.J. A continuum mechanics based four-node shell element for general non-linear analysis. Eng. Comput, 1(1), p.77-88, 1984. https://doi.org/10.1108/eb023562.
14. Bathe K.J., Dvorkin E.N. A form. of general shell elements – the use of mixed interpolation of tensorial components. Int J Num Met Eng, 22(3), p.697-722, 1986. https://doi.org/10.1002/nme.1620220312.
15. Bathe K.J., Dvorkin E.N. A four-node plate bending element based on Mindlin-Reissner plate theory and a mixed inter. Int J Num Met Eng, 21, p.367-383, 1985. https://doi.org/10.1002/nme.1620210213.
16. Lardeur P. Développement et évaluation de deux nouveaux éléments finis de plaques et coques composites avec influence du cisaillement transversal. Thèse UTC, 1990.
17. Batoz J L, Dhatt G. Modélisation des structures par élément finis. Volume 2: Poutres et plaques, Hermes, Paris, 1990.
18. Katili I. An improved incompatible DSQ element using free formulation approach. Struc Eng and Mech, 78(6), p.665-679, 2021. https://doi.org/10.12989/sem.2021.78.6.665.
19. Katili I., Batoz J.L, Maknun I.J., Lardeur P. A comparative formulation of DKMQ, DSQ and MITC4 quadrilateral plate elements with new numerical results based on s-norm tests. Comput. Struct, 204, p.48-64, 2018. https://doi.org/10.1016/j.compstruc.2018.04.001.
20. Katili I., Batoz J.L., Maknun I.J., Katili A.M. On static and free vibration analysis of FGM plates using an efficient quadrilateral finite element based on DSPM. Compos Struct, 261, p.1-19, 2021. https://doi.org.10.1016/j.compstruct.2020.113514.
21. Maknun I.J., Natarajan S., Katili I. Appilcation of discrete shear quadrilateral element for static bending, free vibration and buckling analysis of functionally graded material plate. Compos Struct, 284, p.115-130, 2022. https://doi.org/10.1016/j.compstruct.2021.115130.
22. Srinivas S. A refined analysis of composite laminates. J Sound Vib, 30(4), p.495-507, 1973. https://doi.org/10.1016/S0022-460X(73)80170-1.
23. Pagano N.J. Exact solutions for rectangular bidirectional composites and sandwich plates. J Compos Mater, 4(1), p.20-34, 1970. https://doi.org/10.1177/002199837000400010.
24. Pagano N.J., Hatfield S.J. Elastic behavior of multilayered bidirectional composites. AIAA, 10, p.931-933, 1972. https://doi.org/10.2514/3.50249.
25. Reissner E. The effect of transverse shear deformation on the bending of elastic plates. J Appl Mech Eng ASME, 12, p.69-77, 1945. https://doi.org/10.1115/1.4009435.
26. Mindlin RD. Influence of rotation inertia and shear on flexural motion of isotropic elastic plates. J Appl Mech, 18, p.31-38, 1951. https://doi.org/10.1115/1.4010217.
27. Katili I., Maknun I.J., Batoz J.L., Katili A.M. Asymptotic equivalence of DKMT and MITC3 elements for thick composite plate. Comp Str, 206, p.363-379, 2018. https://doi.org/10.1016/j.compstruct.2018.08.017

28. Maknun I. J., Yvas A. Effect of Mesh Orientation on Accurate Solution in Static Analysis of Composite Plate Structures. Evergreen, 11, p.3325-3332, 2024. https://doi.org/10.5109/7326967
29. Katili I., Maknun I.J., Katili A.M., Bordas S.P.A., Natarajan S. A unified polygonal locking-free thin/thick smoothed plate el. Com Str, 2019, p.147-157, 2019. https://doi.org/10.1016/j.compstruct.2019.03.020.
30. Katili I., Maknun I.J., Millet O., Hamdouni A. Application of DKMQ element for composite plate bending structures. Compos Struct, 132, p.166-174, 2015. https://doi.org/10.1016/j.compstruct.2015.04.051.